

AD/A-004 987

STUDIES OF SEA-STATE EFFECTS ON ANTENNAS
IN SHIPBOARD COMMUNICATIONS SYSTEMS

Richard W. Adler, et al

Naval Postgraduate School

Prepared for:

Naval Electronic Systems Command

August 1974

DISTRIBUTED BY:

NTIS

National Technical Information Service
U. S. DEPARTMENT OF COMMERCE

UNCLASSIFIED

SECURITY CLASSIFICATION OF THIS PAGE (When Data Entered)

ADJ/004987

REPORT DOCUMENTATION PAGE		READ INSTRUCTIONS BEFORE COMPLETING FORM
1. REPORT NUMBER NPS - 52Ab74081	2. GOVT ACCESSION NO.	3. RECIPIENT'S CATALOG NUMBER UNCLASS
4. TITLE (and Subtitle) Studies of Sea-State Effects on Antennas in Shipboard Communications		5. TYPE OF REPORT & PERIOD COVERED Final Report Sept 1969 - Dec 1971
		6. PERFORMING ORG. REPORT NUMBER
7. AUTHOR(s) Richard W. Adler George A. Rahe		8. CONTRACT OR GRANT NUMBER(s) NAVELEX PME 117 X1508(T)
9. PERFORMING ORGANIZATION NAME AND ADDRESS Naval Postgraduate School Monterey, CA 93940 Code 52Ab		10. PROGRAM ELEMENT, PROJECT, TASK AREA & WORK UNIT NUMBERS PO 0-4520
11. CONTROLLING OFFICE NAME AND ADDRESS Naval Electronics Systems Command PME-117 Washington D.C. 20362		12. REPORT DATE August 1974
		13. NUMBER OF PAGES
14. MONITORING AGENCY NAME & ADDRESS (if different from Controlling Office)		15. SECURITY CLASS. (of this report) Unclassified
		15a. DECLASSIFICATION/DOWNGRADING SCHEDULE
16. DISTRIBUTION STATEMENT (of this Report) Approved for public release; distribution unlimited.		
17. DISTRIBUTION STATEMENT (of the abstract entered in Block 20, if different from Report)		
18. SUPPLEMENTARY NOTES Reproduced by NATIONAL TECHNICAL INFORMATION SERVICE U.S. Department of Commerce Springfield, VA. 22151		
19. KEY WORDS (Continue on reverse side if necessary and identify by block number) Antennas Shipboard Sea-State		
20. ABSTRACT (Continue on reverse side if necessary and identify by block number) The effect of sea surface conditions on the performance on antennas in VLF, HF and VHF shipboard communications is addressed. In the VLF range, towed buoyant cables are examined. The equations of force are derived & presented and the towed cable configuration is simulated on a hybrid computer. A method of calculating the received voltage is developed. The complexity of simulating a cable antenna in a real-world sea surface environment is addressed.		

DD FORM 1473

1 JAN 73

EDITION OF 1 NOV 65 IS OBSOLETE
S/N 0102-014-66011

UNCLASSIFIED

SECURITY CLASSIFICATION OF THIS PAGE (When Data Entered)

(item # 20 continued)

HF shipboard antennas used in ionospheric communications systems are simulated on the hybrid computer and the effect of sea state is determined by calculating the time varying gain pattern of the antennas. Recommendations for antenna types which are less sensitive to sea state are made.

A similar simulation conducted for a VHF radiator on a ship in typical sea conditions is compared with measured received signals.

TABLE OF CONTENTS

Form DD 1473

Section I - Feasibility Study for the Simulation.....	3
of Floating Wire Antennas in Presence of Rough Seas	
I. INTRODUCTION.....	3
II. HYDRODYNAMICS OF BUOYANT CABLE.....	4
A. Basic Geometry and Forces.....	6
B. Drag Force Considerations.....	6
C. Cable Equations.....	14
D. Force Effects of Waves on the Floating Cable.....	16
III. COMPUTER SIMULATION OF CABLE.....	18
A. System Description.....	18
B. Computer simulation.....	21
C. Discussion.....	23
D. Conclusions.....	23
E. Recommendations.....	23
IV. FORMULATION OF RECEIVED SIGNAL VOLTAGE.....	25
ON BUOYANT CABLE	
A. Water Wave Effects on Electromagnetic Fields.....	25
Beneath the Ocean Surface.	
B. Received Voltage Equations.....	26
V. SUMMARY AND RECOMMENDATIONS.....	30
REFERENCES.....	33
Section II - Sea State Effects on HF Ionospheric Communi-... 34	
cations Circuits	
I. INTRODUCTION.....	34
II. COMPUTER SIMULATION.....	35
III. CONCLUSIONS AND RECOMMENDATIONS.....	39
REFERENCES.....	41

Section III - Sea State Effects on Shipboard VHF.....	49
Antenna Patterns	
I. INTRODUCTION.....	49
II. THEORY OF THE PROBLEM.....	50
A. Simple Antenna Over Ground.....	50
B. Rotation of the Antenna.....	51
C. Effects of a Rough Ground Plane.....	52
D. The Sea as a Ground Plane.....	53
E. The Composite Picture.....	54
III. EXPERIMENTAL PROCEDURES.....	55
A. Equipment Setup.....	55
IV. EXPERIMENTAL RESULTS.....	57
A. Recorded Data.....	57
B. Computer Simulations.....	59
V. COMPARISON OF RESULTS.....	60
A. Distributional Analysis.....	60
B. Variational Analysis.....	60
C. Simulation Analysis.....	60
VI. CONCLUSIONS.....	64
INITIAL DISTRIBUTION LIST.....	65

S E C T I O N I

Feasibility Study for the Simulation of Floating Wire Antennas in Presence of Rough Seas

I. INTRODUCTION

Survivable VLF communications systems under development by the Navy all include the use of submarine antennas in the form of towed buoyant cables. One unknown factor which will affect the performance of these systems is the phase and amplitude variations of signals, as received by the floating antenna, caused by sea surface conditions.

In the ideal zero sea-state condition, the towed cable antenna will have a portion (at least 100 feet) of its length floating on the surface. This exposed portion is responsible for virtually all of the voltage delivered to the receiver. The major portion of the antenna length is submerged and the fields reaching these submerged portions will be attenuated and phase shifted by the sea water. When the sea surface contains waves, the surfaced portion of the antenna may not be entirely floating, but could be partly exposed and partly under the local water waves.

Some method of estimating the effects of wave motion on received signals is needed before system performance can be predicted for all operation environments. One approach to

the problem is to develop a simulation model of the submarine antenna and sea surface. If an analog or hybrid computer could be programmed to calculate the cable location for assumed sea surface conditions, it should be possible to calculate the phase & amplitude of signals intercepted by the conductor. The Naval Postgraduate School's study of this possibility is the subject of this section.

II. HYDRODYNAMICS OF BOUYANT CABLE

A. BASIC GEOMETRY AND FORCES

The basic theory for a bouyant cable which is towed by a submarine is contained in a report by Pode. [1] The standard assumptions of single plane geometry and straight-line motion of the sub are made. Figure 1 illustrates the coordinate system and variables.

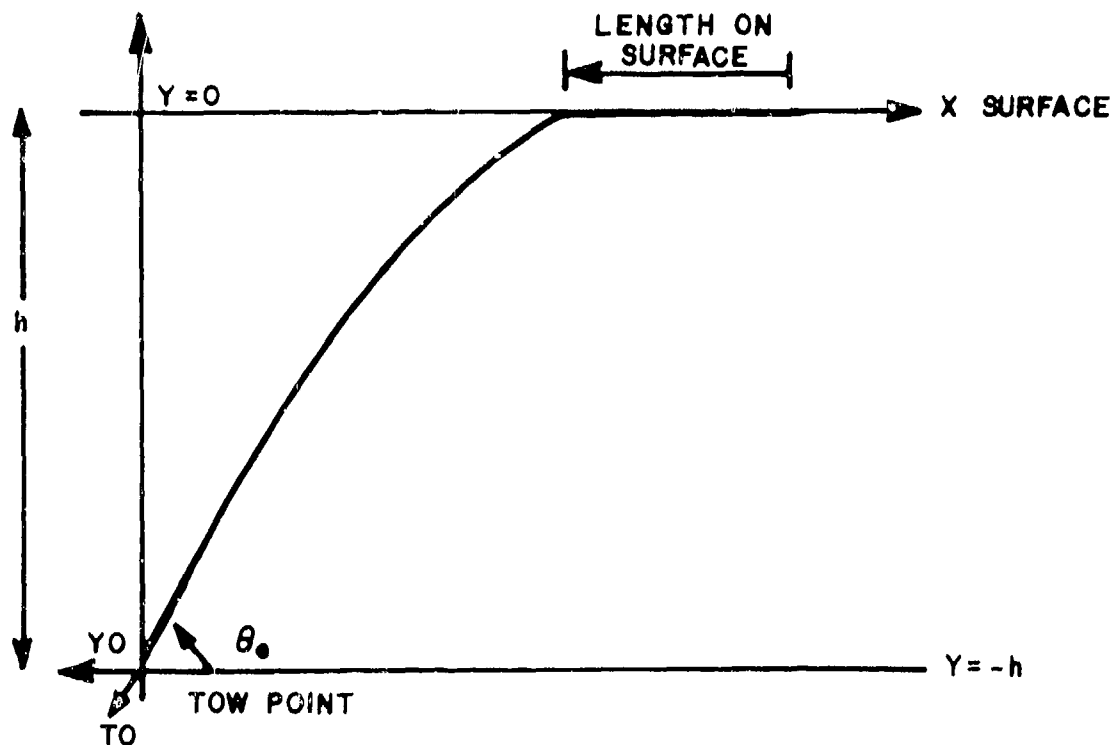


FIGURE 1. TOWED BOUYANT CABLE

A differential element is next considered, and the various forces acting on it are noted.

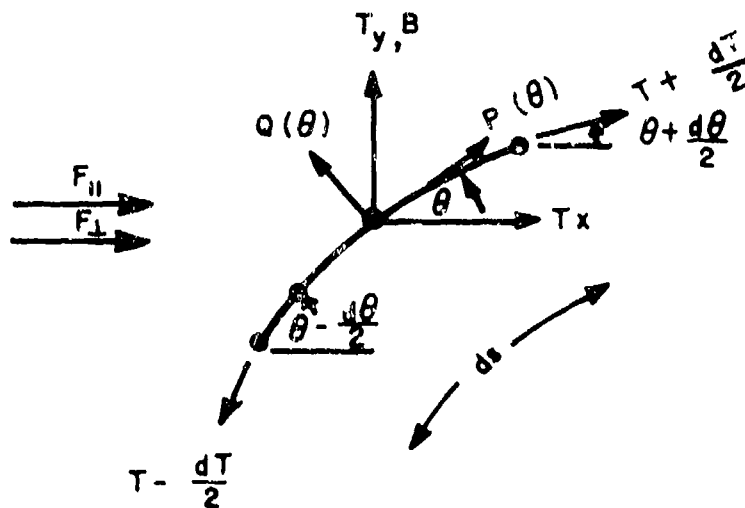
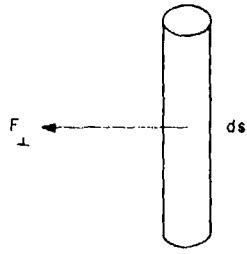


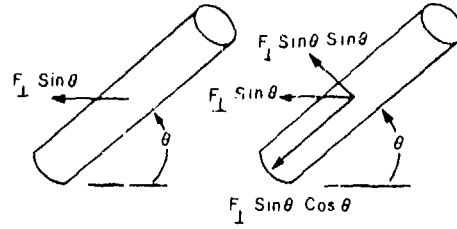
FIGURE 2. DIFFERENTIAL CABLE ELEMENT

- F_{\parallel} = Drag/unit length when cable is parallel to stream
- F_{\perp} = Drag/unit length when cable is perpendicular to stream
- B = Bouyancy weight/unit length ($B=0, y \geq 0$)
- $P(\theta)$ = Parallel forces acting longitudinally on cable
- $Q(\theta)$ = Quadrature forces acting transversly on cable
- T = Tension force with x and y components

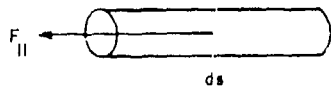
It is readily seen that the P & Q forces and T_x & T_y tensions can be expressed in terms of the drag forces and bouyant force. the following sequence of diagrams show the drag forces resolved into componenets both parallel and perpendicular to the cable.



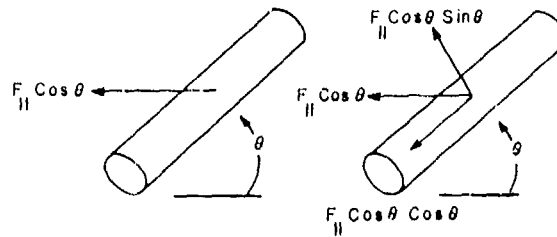
a. Cable Perpendicular to Stream Motion



b. Cable Off-Perpendicular to Stream Motion



c. Cable Parallel to Stream Motion



d. Cable Off-Parallel to Stream Motion

Figure 3 Resolution of Drag Forces

B. DRAG FORCE CONSIDERATIONS

The determination of cable configuration in the presence of surface waves is solely a matter of keeping close track of all the drag force components. Previously, analysis of cable configuration did not include minor force terms and assumed perfectly smooth cables. This was justified for zero sea-state conditions since the cable calculations were for the purpose of estimating the amount of cable reaching the surface. However, when waves are present, crests and troughs

apply local forces which tend to force the cable deeper or else bouy it up out of the water. The effects to be presented next will have to be included in any simulation involving wave effects. [2]

1. Normal Drag.

This component is also called Pressure Drag, Perpendicular Drag or Resistance. The equation relating normal drag to body shape, fluid density, velocity and drag area is:

$$D = C_d \frac{\rho}{2} V^2 A, \text{ where}$$

D is the normal drag force.

C_d is the coefficient of drag for the body shape

ρ is the fluid density

V is the stream velocity and

A is the drag area.

For a smooth cylinder, experimental determination of drag coefficient is made versus the Reynolds Number, R_d , which represents the ratio of drag to friction forces.

$$R_d = \frac{Vd}{\nu} \quad \text{where } \nu = \text{Kinematic viscosity}$$

of the fluid. For seawater, $\nu \approx 1.5 \cdot 10^{-5}$ ft²/ sec.

If surface roughness exists, even in an amount as small as 2% of the cable diameter, the drag coefficient changes abruptly for high Reynolds numbers. Figure 4 demonstrates this.

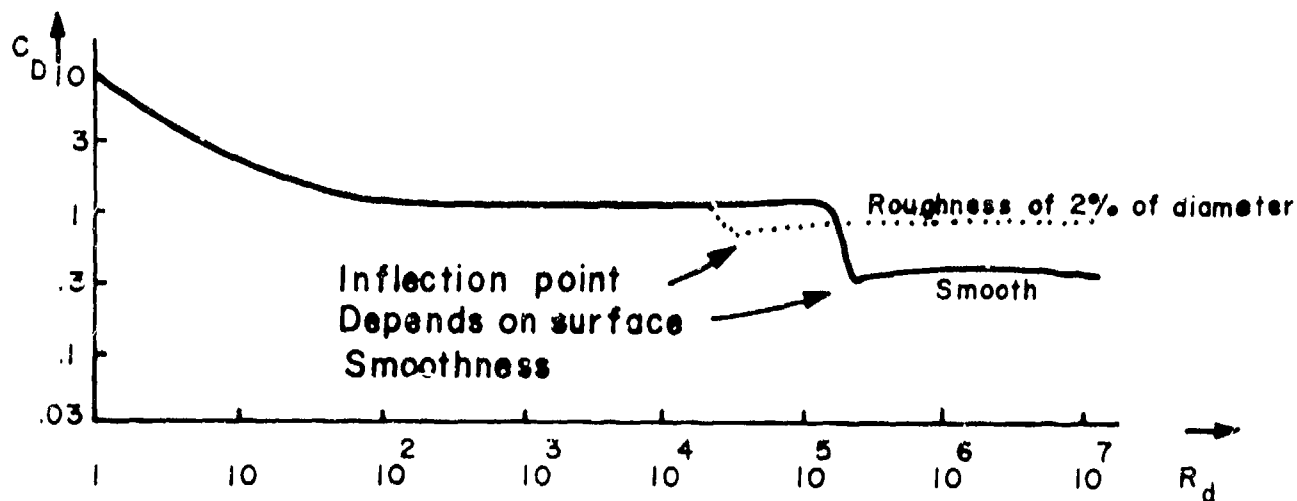


Figure 4 Drag Coefficient for Smooth Cylinder

To establish values of C_D which apply for our situation, consider this example:

$$V = 10 \text{ knots}$$

$$\rho = 2 \text{ lb. sec}^2/\text{ft}^4$$

$$R_d \leq 10^5 \text{ and for a smooth cable,}$$

$$C_D \approx 1 \text{ to } 1.5$$

If the cable has surface wrinkles of 0.01 inches, the C_D could drop from 1.2 to .3.

Conclusion: C_d values of from 1.2 to .3 should be used until exact values of surface roughness can be established.

2. Parallel Drag.

This part of cable drag is sometimes called tangential drag or skin friction drag and is proportional to the same type of parameters as normal drag.

$$D = \left(\frac{C_f}{C_T} \right) \frac{P}{2} V^2 \quad \text{where}$$

C_T is a local value of the coefficient of friction drag and C_f is an average value of the coefficient of friction drag.

$$C_T = \frac{d C_f}{d \left(\frac{R_x}{R_\ell} \right)} \quad \text{where } \ell \text{ is the width under drag and}$$

x is the distance from the leading edge to the observation point.

A laminar boundary layer starts at the leading edge of the body (and has a C_T associated with it) and soon gives way to a turbulent boundary layer at the critical Reynolds number of approximately 3×10^5 to 5×10^5 . Figure 5 illustrates this for a long thin cylinder. It has been determined that for $R \leq 10^6$ (valid for this study),

$$C_T = \frac{.06}{R_x^{1/5}} \quad \text{and} \quad C_f = \frac{.07}{R_\ell^{1/5}}$$

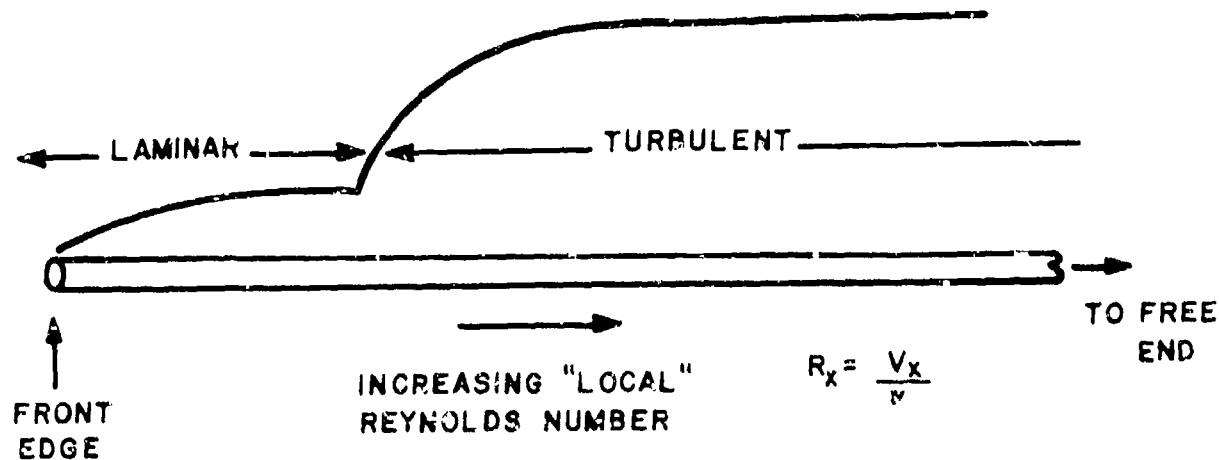


Figure 5 Laminar and Turbulent Flow

The laminar region is quite short for towed cables:

If $V = 10$ knots, R_x critical $\approx 4 \times 10^5$ which yields $x = 3$ inches for typical cables.

For seawater,

$$R_x = 1.6 \times 10^5 \text{ per ft-knot}$$

Above $R = 10^6$,

$$C_f = \frac{.44}{R_x^{1/6}}, \quad C_\tau = \frac{.036}{R_x^{1/6}}$$

These values of C_f and C_τ are valid for normal cable lengths;

at 10 knots and for 1000 ft.,

$$R_x = 1.6 \times 10^8 .$$

3. Pressure Drag on Inclined Cable.

When the cable is tilted with respect to the stream velocity, the drag coefficient, C_d , must be resolved

into two components, horizontal and vertical. Experimental verification has justified Figure 6 for values below the critical Reynolds number.

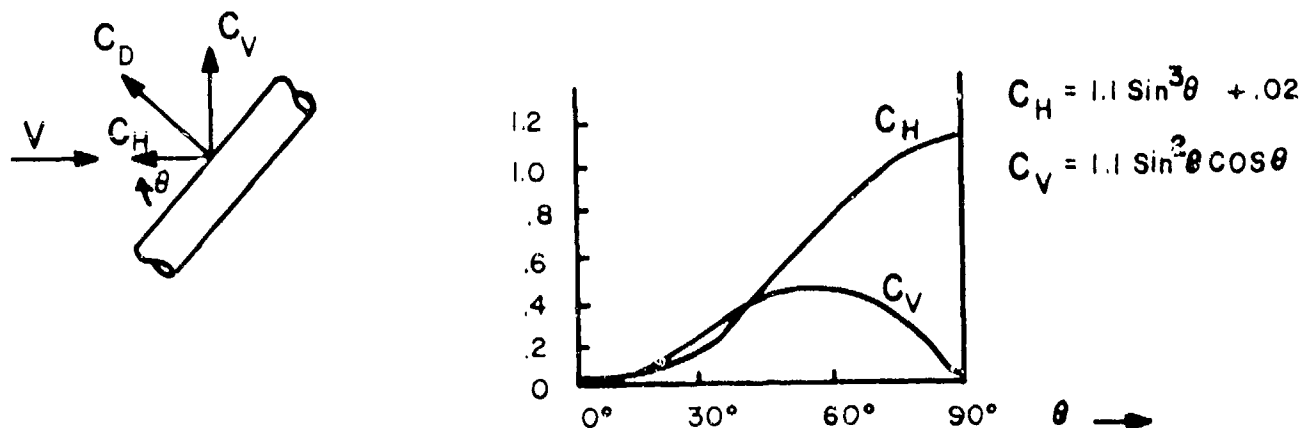


Figure 6 Pressure Drag Components on Tilted Cable

Note that the use of C_V and C_H implies V is the stream velocity. The $\sin^2 \theta$ term in C_H accounts for the perpendicular component of velocity (which contributes to C_D) and the additional $\sin \theta$ gives the C_H component of C_D . Similarly for the equation for C_V . The .02 constant term is an average friction term for the experiment.

4. Drag Force Summary

For pressure drag, cable is considered either smooth or rough.

a. Smooth cable

$$C_d \approx 1.1, R_d \leq 10^5$$

$$C_d \approx 0.4, R_d > 10^5$$

$$C_v = C_d \sin^2 \theta \cos \theta$$

$$C_h = C_d \sin^3 \theta$$

b. Rough cable

Choose a "jump point" in C_d for the value of R_d from Figure 7, depending on the best estimate of cable roughness.

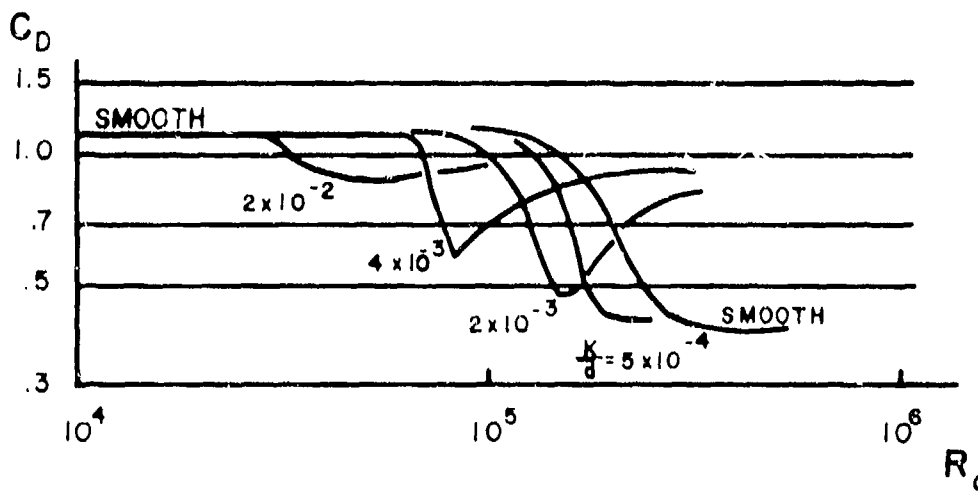


Figure 7 C_d for Various Roughness Factors

For friction drag, consider turbulent drag along the entire cable. From the following examples,

$$C_f = .025$$

for various lengths of cable and velocities. As an initial effort, a "residual" value of .025 can be added to the value of C_h .

Example:

5 Knots (8 ft./sec.)

500 ft. of $\frac{1}{2}$ in. diameter cable.

$$R = \frac{V}{\ell v} \quad R_x = \frac{V}{xv}$$

$$\ell = \pi d$$

$$R_\ell = \frac{8 \text{ ft./sec.}}{\frac{1.5 \text{ in}}{12 \text{ in/ft}}} = 1.5 \times 10^{-5} \text{ ft}^2/\text{sec} = 4.3 \times 10^6$$

$$R_x = \frac{8 \text{ ft./sec}}{500 \text{ ft} \times 1.5 \times 10^{-5} \text{ ft}^2/\text{sec}} = 1.08 \times 10^3$$

$$C_r = \frac{.06}{R_x^{1/5}} = .015$$

$$C_f = \frac{.44}{R_\ell^{1/6}} = .035$$

} at 500' along the cable

At 50 ft. along the cable,

$$R_x = \frac{g}{50 \times 1.5 \times 10^{-5}} = 1.08 \times 10^4$$

$$C_r = .0094$$

Thus the coefficient of friction drag is about 0.025 for typical velocities and lengths.

C. CABLE EQUATIONS

Referring to Figures 1 and 2, a force balance equation shows:

$$dT = -Pds$$

$$Td\theta = -Qds$$

At tow point, T_0 and θ_0 are limiting values.

Dividing,

$$\frac{dT}{T} = \frac{P}{Q} d\theta$$

$$\frac{T}{T_0} = e^{\int_{\theta_0}^{\theta} \frac{P}{Q} d\theta}$$

$$ds = \frac{T_0}{-Q} e^{\int_{\theta_0}^{\theta} \frac{P}{Q} d\theta} d\theta$$

$$s = \int_{\theta_0}^{\theta} \frac{T_0}{-Q} e^{\int_{\theta_0}^{\theta} \frac{P}{Q} d\theta} d\theta$$

$$dx = \cos \theta ds$$

$$dy = \sin \theta ds$$

For the x and y components of tension,

$$dT_x = (-Pds)_x + (-Qds)_y = -P\cos\theta ds + Q\sin\theta ds = -Pdx + Qdy$$

$$dT_y = (-Pds)_y + (-Qds)_x = -P\sin\theta ds - Q\cos\theta ds = -Pdy - Qdx$$

Using values for P and Q from Figure 3,

$$P(\theta) = -F \cos^2\theta - F \cos\theta \sin\theta + B \sin\theta$$

$$Q(\theta) = F \cos\theta \sin\theta + F \sin^2\theta + B \cos\theta$$

Each of the F terms are calculated from cable parameters and local stream velocities. For zero sea-state, these equations were programmed. If a rough sea surface is assumed, the equations for the water waves must be formulated and solved to provide local stream velocities which can then be used for evaluating localized F's.

When F's are found and substituted into the above expressions for P and Q, and the cable equations are themselves solved, the location of each point on the cable will be known for that instant of time. This information, together with a knowledge of the location of the local water surface points at that same time will enable the calculation of received voltage at the submarine from a chosen radio wave field configuration.

The complexity of the problem is beginning to be obvious, even without knowing, at this point, the methods available for estimating sea surface and for calculating the electric field which penetrates the water and induces a voltage on the cable antenna.

D. FORCE EFFECTS OF WAVES ON THE FLOATING CABLE

The bouyant cable, in a zero sea-state ocean will have its surfaced portion lying partly submerged in the water & partly exposed. Only vertical bouyancy force & parallel drag act on the cable. If low steepness waves are present, with sufficient bouyancy the cable will follow the surface wave profile. When the wave period becomes less & the steepness increases, the cable will not necessarily follow the profile.

Two additional effects come into play here.

1. The cable will tend to be forced downward by additional tension forces at wave crests & upward at troughs.



Figure 8 Cable Forces on Waves Crests & Troughs

2. The internal water particle motion beneath the surface creates a local circulatory force, as seen in Figure 9.

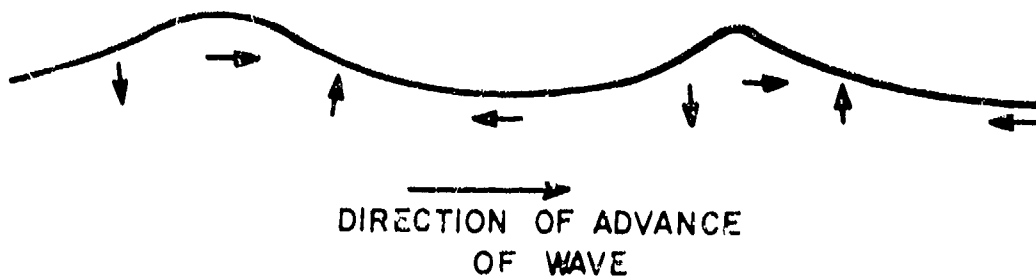


Figure 9 Direction of Motion of Water Particles
in a Wind Wave

This circular force produces localized pressure and friction drag components superimposed on the previous zero sea-state forces.

The above simplified picture is for a non-existent single-frequency idealized wave. The typical ocean wave environment is a massive collection of many simple waves plus individual localized hillocks of water which move independently of each other. Words such as period, frequency, velocity and wavelength lose their meaning at sea. Statistical descriptions are the only method of gaining some insight as to what a typical ocean waves might be like. [3,4]

III COMPUTER SIMULATION OF CABLE

A. SYSTEM DESCRIPTION

The system as described below permits a closed-form solution requiring no iterative techniques. The computational starting point is the transition point between the surface portion of the cable, the point labeled "T" is Figure 10.

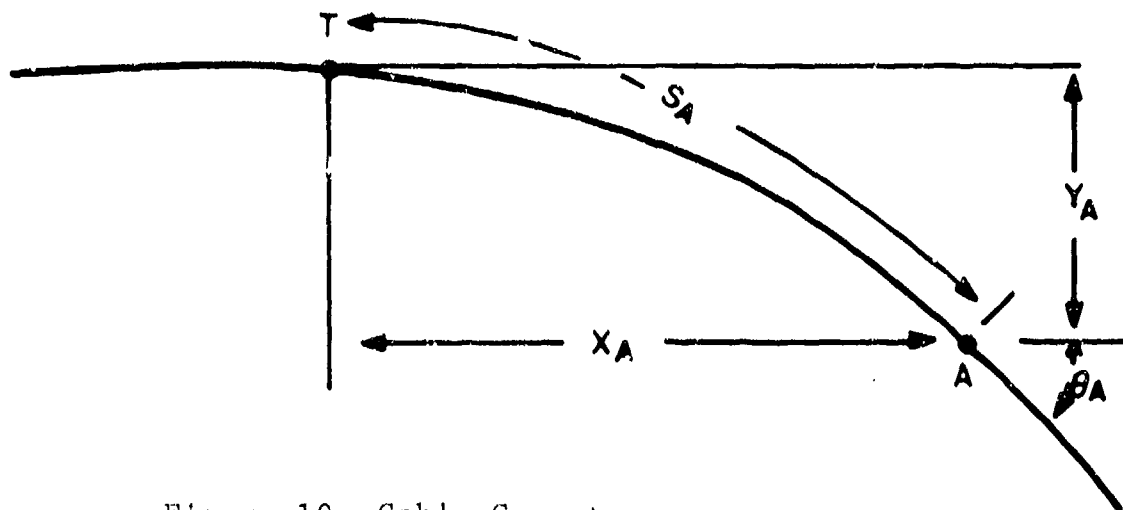


Figure 10. Cable Geometry

The horizontal component of the cable tension at a point A on the submerged portion is:

$$T_x(S_A) = T_{x0} + \int_0^{S_A} C_{hd} V^2 ds$$

where T_{x0} is the drag force due to the surface portion

The vertical component is:

$$T_y(S_A) = T_{y0} + \int_0^{S_A} (-B + C_{vd} V^2 d) ds$$

where $T_{y0} = 0$

The parameters in these equations are described below:

$d = .65$ inches, cable diameter

$B = (\rho_{sw} - \rho_c)A_c$, cable buoyancy

$\rho_{sw} = 64.9$ lbs/ft³, sea-water density

$\rho_c = \rho_w \times G_c$

$\rho_w = 62.4$ lbs/ft³, fresh-water density

$G_c = .78$, cable specific gravity

A_c is cable cross-sectional area

$$\text{So, } B = [64.0 - 0.78(62.4)] \left[\frac{\pi(0.65)^2}{4(144)} \right]$$

$$= .035 \text{ lb/ft}$$

The distances X_A and Y_A and the angle θ_A are:

$$X_A = \int_0^{S_A} \cos\theta \, ds$$

$$Y_A = \int_0^{S_A} \sin\theta \, ds$$

$$\theta_A = \tan^{-1} \left[\frac{T_y(S_A)}{T_x(S_A)} \right]$$

The submerged portion of the cable is described,
then by the following equations:

$$\frac{d T_x}{ds} = C_{hd} v^2 d \quad (1)$$

$$\frac{d T_y}{ds} = -B + C_{vd} V^2 d \quad (2)$$

$$\frac{dx}{ds} = \cos \theta$$

$$\frac{dy}{ds} = \sin \theta$$

$$\tan \theta = \frac{T_y}{T_x}$$

$$C_{hd} = 1.1 \sin^3 \theta + 0.22$$

$$C_{vd} = 1.1 \sin^2 \theta \cos \theta$$

The distances X_A and Y_A and the angle θ_A are:

$$X_A = \int_0^{S_A} \cos \theta \, ds$$

$$Y_A = \int_0^{S_A} \sin \theta \, ds$$

$$\theta_A = \tan^{-1} \left[\frac{T_y(S_A)}{T_x(S_A)} \right]$$

The submerged portion of the cable is described, then, by the following equations:

$$\frac{dT_x}{dx} = C_{hd}V^2d \quad (1)$$

$$\frac{dT_y}{ds} = -B + C_{vd}V^2d \quad (2)$$

$$\frac{dx}{ds} = \cos\theta$$

$$\frac{dy}{ds} = \sin\theta$$

$$\theta = \tan^{-1} \left[\frac{T_y}{T_x} \right]$$

B. COMPUTER SIMULATION

The diagram shown in Figure 11 was implemented on a Comcor Ci-5000 analog computer to simulate the system described by equations (1) and (2), with computation time of 1 second corresponding to 100 feet of cable.

The functions $500\sin\theta$ and $5000(1-\cos\theta)$ were generated by diode function generators for the range $0 \leq \theta \leq 10^\circ$.

The following parameters were recorded during computation on an eight-channel recorder (Brush model Mark 200):

$$\frac{s}{20}, \frac{y}{20}, -\frac{x}{20}, \frac{T_x}{10}, \frac{T_y}{2}, 500 \frac{T_y}{T_x}$$

The "y vs x" curve was also monitored on the Ci-5000's oscilloscope.

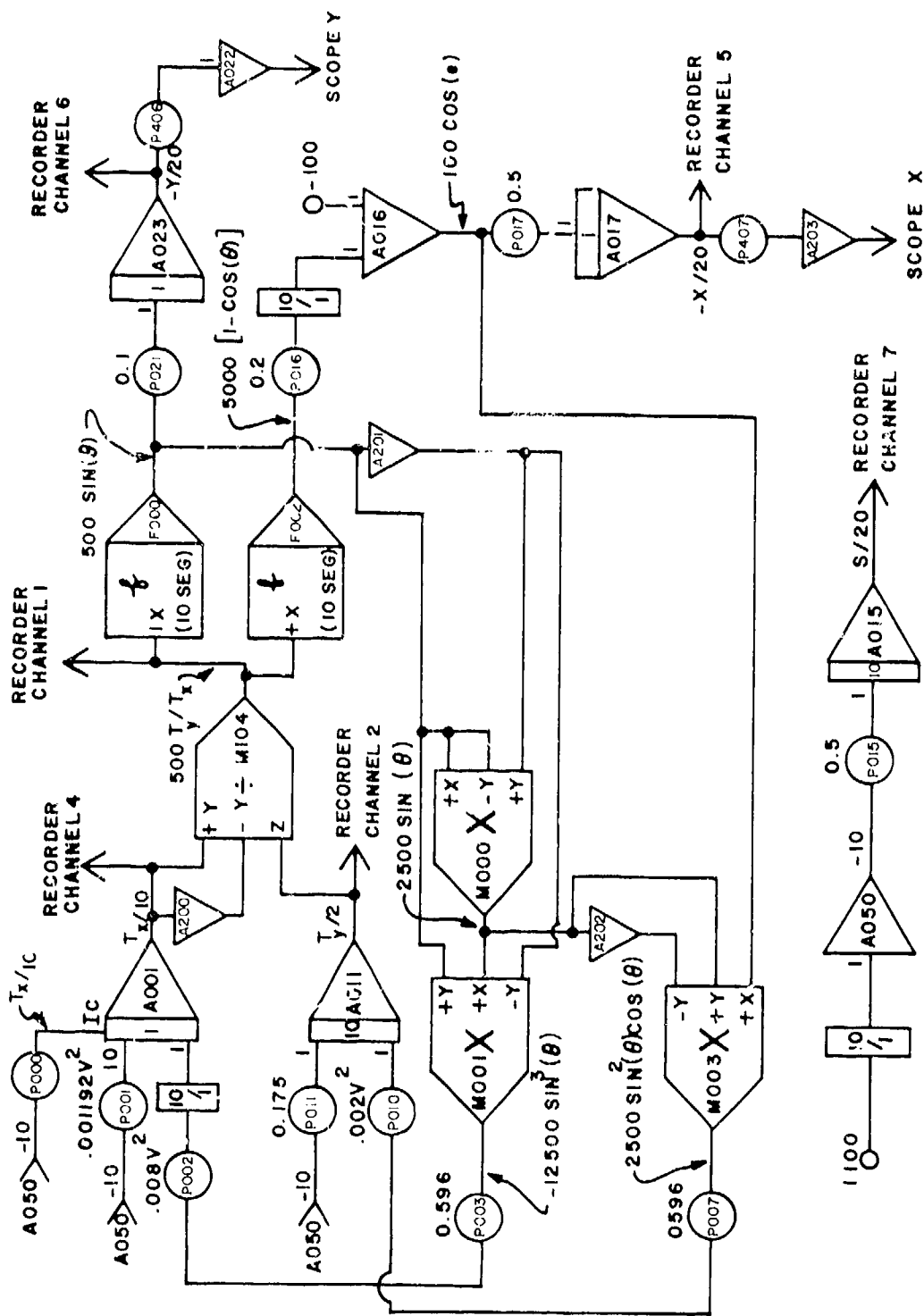


FIGURE II - ANALOG CIRCUIT DIAGRAM

C. DISCUSSION

Using the simulation described, it was possible, for any specified towing velocity and surface cable length, to obtain in a single continuous computation the geometrical cable configuration and cable tension over the depth-range of interest.

It would have been possible, also, to have studied the effect of changing any of the several drag coefficients from the assumed values. Further, the cable diameter and/or cable specific gravity could be modified and results thus obtained for different cable types.

It must be noted that no effort was made to include the effects of rough seas on the cable.

D. CONCLUSIONS

1. A closed-form solution was developed for cables towed by submarines as a function of velocity and length of cable on the surface for the case of a flat sea.

2. The simulation of a statistically significant surface is extremely complex and subject to a large number of variables.

E. RECOMMENDATIONS

1. Confirmation of the mathematical model of the behavior of the cable's submerged portion could be obtained by towing a cable from a submerged boom from a surface craft. This would provide sufficient data without requiring

difficult-to-obtain submarine services.

2. It is felt that the surface behavior of the cable for varying sea states could be similarly obtained and the resulting horizontal tension then used as an input to the model that has been presented here.

3. Plots relating the relationships among cable type, towing velocity, submarine depth and cable length could be readily obtained by expanding the simulation into a hybrid simulation.

IV FORMULATION OF RECEIVED SIGNAL VOLTAGE ON BUOYANT CABLE

It is expected that the largest portion of received signal will come from the exposed portion of the cable. For submerged lengths, both amplitude and phase shift changes with depth are well-known for plane, zero sea-state conditions [5]. A previously uncertain perturbation to the idealized electric field just mentioned could be from waves which produce locally varying depths at the cable sections under consideration. It, thus, might be possible that wave action-induced amplitude and phase variations would have to be added to depth variations already known.

A. WATER WAVE EFFECTS ON ELECTROMAGNETIC FIELDS BENEATH THE OCEAN SURFACE

An analysis was done for the case of a sinusoidally varying ocean surface and a downward traveling vertically polarized wave. Since the radio wavelength is much greater than the water wavelength, a quasi-static approximation can be made. The wave equation solution, subject to usual boundary conditions, must be periodic in the direction of the water wave propagation. Applying the Method of Moments reduces the problem to a system of linear algebraic equations which can be solved by matrix techniques.[6] Results show that no appreciable difference (less than 1% amplitude and 1° phase) occurs at depths of interest due to the sinusoidal

shape of the surface. Thus, the only important parameter to be considered is local depth for the differential length of cable under consideration.

B. RECEIVED VOLTAGE EQUATIONS

The calculation of the received voltage is accomplished by integrating or summing the differential induced voltages which occur at each position along the cable from the surfaced sea-ground end to the submerged tow point, which is effectively terminated in an open circuit. A transmission line approach is valid for transferring the voltage from its point of induction to the receiver terminals.

Three regions of interest can be identified:

1. The exposed surface portion where the incident value of electric field impinges on the conductor.
2. The covered surface portion or the part which is shallowly covered by wavelets.
3. The submerged portion, whose lower end is sufficiently deep so that it contributes an insignificantly small amount of voltage, but whose upper end must be included.

The differential voltage expressions follow:

1. Exposed Surface Portion:

$$dV(s) = -E(s,d) \Big|_{d=0} ds = -E(s,o) ds$$

where $E(s,o)$ is the horizontally polarized incident

field component parallel to the cable. Here, d , the depth is taken as zero, and s is the distance along the cable.

2. Covered Surface Portion:

$$dV(s) = -E(s,d)ds$$

where $E(s,d) = E(s,0) e^{-\gamma d}$, $\gamma =$ propagation constant for seawater

When water waves cover part of the surfaced portion, d is a function of s and time, that function being determined a priori by some method of predicting the wave profile.

3. Submerged Portion:

$$dV(s,d) = -E(s,d) ds = -E(s,0) \cos\theta e^{-\gamma d} ds$$

The $\cos\theta$ term adjusts for the cable inclination of the submerged portion. See Figures 1 and 2. The lower end, it was mentioned, will experience only a minute pickup due to the seawater attenuation and phase constants of 1.5db/ft. and $15^\circ/\text{ft}$.

The above differential expressions, can be written as a single term adapted for each of the three regions.

$$dV(s,d) = -E[s,d(s)]ds$$

where $d(s)$ is the local depth of the differential segment, ds . $d(s) = 0$ for the exposed part

$d(s) = S_g \cos\theta$ for the submerged part, as seen in Figure 12.

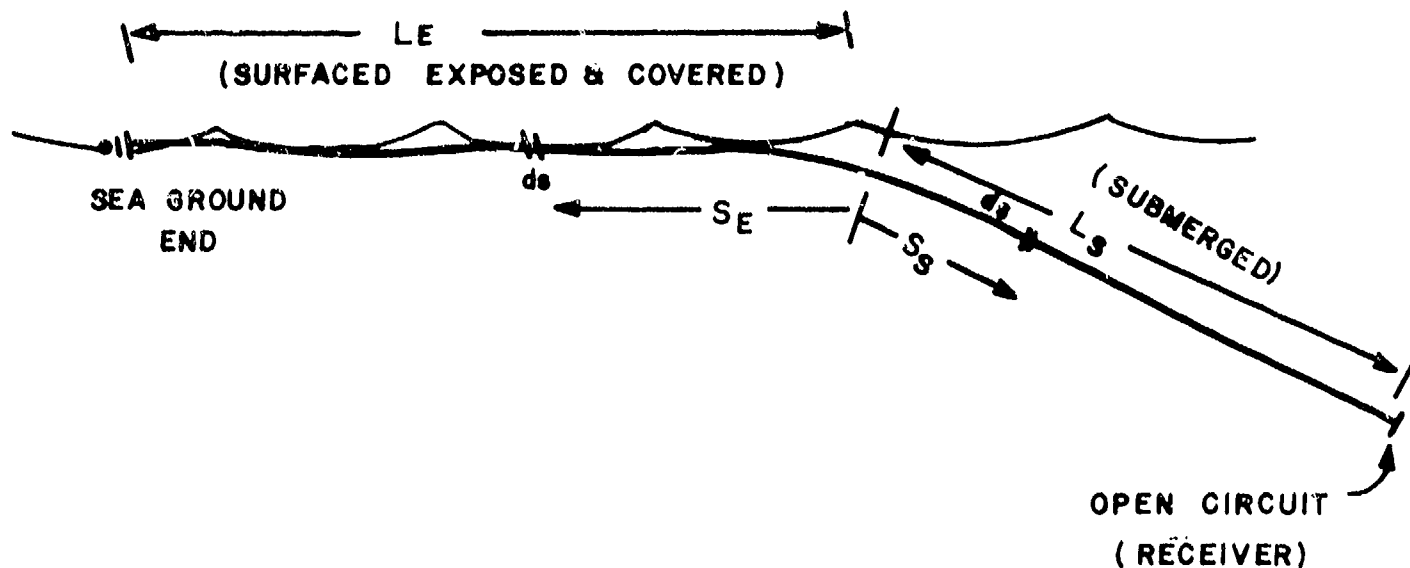
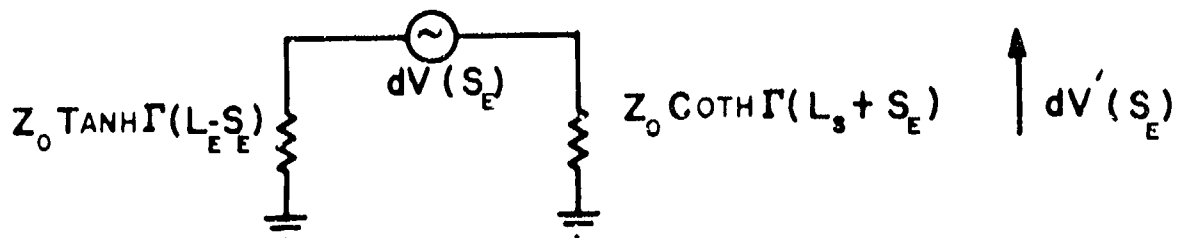


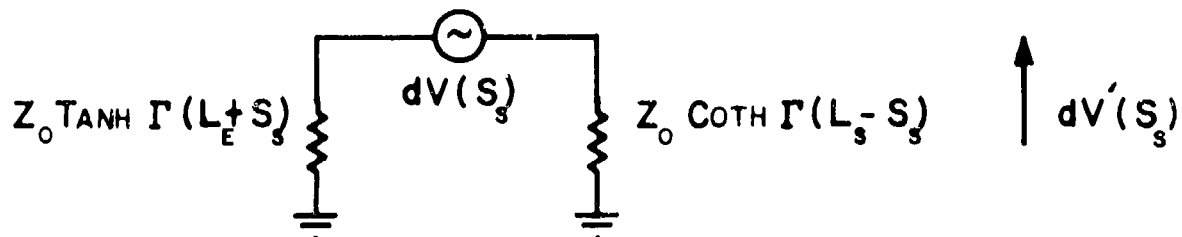
Figure 12. Distance Nomenclature for Cable

Following conventional transmission line nomenclature, equivalent circuit representations for the surfaced and submerged portions are:

1. Surfaced Voltages



2. Submerged Voltages



The open-circuit voltage at the towed end caused by dV' is:

$$dV_{oc} = \frac{dV'(S_E)}{\cosh \Gamma(L_S + S_E)}$$

and
$$dV_{oc} = \frac{dV'(S_S)}{\cosh \Gamma(L_S - S_S)}$$

Substituting the expressions for dV' into the above,

$$dV_{oc} = dV(S_E) \frac{\cosh(L_E - S_E)}{\cosh(L_S + L_E)}$$

and
$$dV_{oc} = dV(S_S) \frac{\cosh(L_E + S_S)}{\cosh(L_S + L_E)} \quad \text{respectively.}$$

The total received voltage is the integral of the two differential voltage expressions over the entire length of the cable. The lower regions of the submerged portion may be neglected once the propagation constants are known.

$$V_{oc} = \int_{S_E=0}^{S_E=L_E} E[S_E, -d(S_E)] \frac{\cosh(L_E - S_E)}{\cosh(L_S + L_E)} dS_E$$

$$+ \int_{S_S=L_S}^{S_S=0} E(S_S, 0) \cos \theta e^{-\gamma S_S \sin \theta} \frac{\cosh(L_E + S_S)}{\cosh(L_E + L_S)} dS_S :$$

The values of $d(S_E)$, θ , L_E AND L_S will depend on the hydrodynamic cable equation solutions, but if they can be obtained, the received voltage V_{oc} can be calculated.

V. SUMMARY AND RECOMMENDATIONS

In all portions of this study, the key parameters needed are the local values of stream velocity for a real-world ocean surface. The motion of the water at, and for shallow depths beneath the surface is absolutely essential for drag force calculation and for received voltage determination.

Only the simplest and most basic ocean model can, at present, be simulated. Indeed, it is possible that we may never be able to satisfactorily determine the desired parameters to great enough accuracy to be able to determine performance effects for the system under consideration.

Previous efforts at calculating the configuration of a towed buoyant cable have assumed zero sea-state, and because of this, were justified in other simplifying approximations concerning drag forces. The more complete drag & cable equations presented in this report should be used if rough sea conditions are included in future work.

The portion of the cable which is exposed, as stated earlier, contributes to the received voltage in a dominant manner. A floating cable of buoyancy 0.7 can be expected to, and will have 30% of its surface exposed to air. That same

cable will, under heavy seas, have slightly less of its surface exposed, on the average, because of the effect of wave crests of adding downward force to the cable. Measurements in the laboratory showed 20% exposed surface.[7] This suggests that the received voltage in heavy seas can be maintained at the zero sea-state level by paying out slightly more cable so as to increase the surfaced amount by one third.

The extreme complexity of determining true wave effects on cable configuration strongly suggests a measurement program be undertaken to collect received voltage versus time for a towed cable. Applying statistical analysis for various cases of sea-state should yield the type of information required for the system simulation. Any attempt to muster up a representable analytic simulation of the cable for real-world sea conditions would result in a computer system of massive size in which the overwhelming majority of hardware and programming would be dedicated to cable equation solutions with a small part of the effort expended on the remainder of the system simulation.

Recommendations are not to pursue the analytical solution for the cable configuration at this time but rather establish via experiment the statistics of received voltage for cases of interest. The experimental output would serve as a base for a simulation model and also might establish insight as to the most important effects of the water waves

on the received signals. After the experiments have been studied, it is entirely possible that a simplified analytic cable solution could be developed that would prove adequate as well as economically attractive.

References

1. Pote, L., "Tables for Computing the Equilibrium Configuration of a Flexible Cable in a Uniform Stream", Navy Department, D.T.M.B. Report 687, March 1951.
2. Hoerner, Fluid Dynamic Drag, 1965.
3. Russell and Macmillan, Waves and Tides, 1970.
4. Bascom, W., Waves and Beaches, 1964.
5. Whalen, et. al., "Experimental Relationships Between VLF Electromagnetic Signal Variations and Water Pressure Variations Caused by Ocean Waves", USNUSL, Report 790., 29 March 1967 (S).
6. Burrows, M.L., "Water-Wave Effects on Radio Wave Propagation in the Ocean", MIT Lincoln Labs, Tech.Note 1970=1, 2 January 1970.
7. Van de Waterling, W.P.M., "The Motion of the Buoyant Antenna Cable RG-298/U at the Ocean Surface", Hydronautics, Inc., T.R. 231-22, June 1968 (S).

S E C T I O N I I

SEA STATE EFFECTS ON HF IONOSPHERIC COMMUNICATIONS CIRCUITS

I. INTRODUCTION

The geometry, hence radiation pattern, of antennas in communications circuits is always assumed to be constant. Shipboard antenna systems have physical geometry that is fixed with respect to the ship, but the ship is in constant motion with respect to an electrical reflecting surface, the ocean. Even the surface of the ocean is in a constant changing state due to sea and wind waves. This section discusses the simplified case of a shipboard antenna, in motion, over a plane, reflecting sea in order to demonstrate the overall effect of sea state on an ionospheric communication system.

Ocean waves cause different types of ship motion; roll, pitch and heave, depending on the particular ship type and its orientation with respect to wave direction. Ship motion may be conveniently resolved into antenna geometry variations in train angle, tilt angle and height. Antenna gain and patterns are highly sensitive to all of these parameters. The gain pattern of a shipboard antenna system is a time-varying function, $G(t, \phi, \theta)$ where ϕ is the observation

azimuth and θ the observation zenith angles. $G(t, \phi, \theta)$ may vary insignificantly during the period of a sea wave or it may undergo very substantial fluctuations. The amount of variation is as dependent on all of the antenna parameters as is the static gain pattern.

The effect of sea conditions on antenna radiation patterns has not been investigated and documented. Variations in signal strength in high seas are commonly acknowledged by communications operators, and may in part be explained by the behavior of the mathematical model of a shipboard antenna system. A quantitative investigation of sea effects has not been undertaken, but presented here are some predicted effects of ship motion in heavy seas on ionospheric communication circuits.

II. COMPUTER SIMULATION

The NPS hybrid graphics - digital computer program GRAPHANT, a computer program for computing and displaying antenna patterns, was used to compute antenna gain patterns on rolling, pitching ships in high sea state conditions.⁽¹⁾ It was modified to calculate roll and pitch of a mine-sweeper size ship from seas of a specified state and wind direction, every 10° of wave period. A new antenna electrical geometry is computed at every increment, and gain patterns for a fixed zenith and azimuth displayed. A "stop action" presentation results, yielding a dynamic pattern variation for

heavy seas. Figures 1 and 2 demonstrate this for a simple vertical whip and horizontal dipole.

To investigate the overall effect of this pattern variation in a practical situation, a specific communications circuit was chosen and calculated. A path length of 1298 KM at 1700 GMT on 15 Jan 1970 was programmed using the ESSA-developed HF ionospheric communications circuit prediction program, HFMUFES.⁽²⁾ The maximum useable frequency for this circuit was 20.3MHz. Several ionospheric modes were possible - a double hop E layer mode and three single hop F layer modes. An azimuth angle of 45° was selected and the appropriate zenith angle for reflection from the ionosphere mode was calculated. Antennas selected were a 10 meter vertical whip and a 7.5 meter horizontal dipole, ship-mounted and subjected to a sea state 5 environment at a bearing of 45° relative. GRAPHANT calculated and recorded the variation of gain at the appropriate zenith angle for each particular mode predicted by HFMUFES. The gain function calculated at each transmission angle varied in time as the waves passed by the ship. The dynamic gain as seen at the ionosphere is different for each mode since a different zenith angle is associated with each mode.

Figures 3 and 4 are plots of the $G(t, \phi, \theta)$ gain function, for each mode, for the vertical whip and horizontal dipole, respectively. Variations range from 2 to 10db and

may be, in a given case, additions to (static) gain, degradations of gain, or periodic variation of gain about a mean value.

Figures 5 and 6 illustrate the ray path for different modes and the gain variation from nominal for each path. Table 1 includes additional data, all for the previously described communications circuit.

Application of these "gain modulations" to propagation predictions can take several forms. The variations may be applied as reliability modifications for heavy weather conditions, but should not be used as enhancement terms since they are rapid variations compared with normal ionospheric fluctuations. They may be applied to signal-to-noise ratios, but again, only degradations should be considered so that predictions will be conservative. A ship motion factor, the range and sense of gain modulation as shown in Table 1, could be developed and applied as the communications system planner sees fit.

The study of the mathematical model is far from complete, however, this initial investigation indicates that some types of $G(t, \phi, \theta)$ variations are typical and may be identified. The variations of Figure 3 are all typical of whips of less than one wavelength with $G(0, \phi, \theta)$ less than the maximum value because the observation (transmission) angles are on the upper side of the lower lobe (see Figure 1). Ship motion causes the lower lobe to fatten and the gain to increase.

The gain variations of Figure 4 show three typical dipole situations. Both lobe shifting and fattening, caused in this instance by height decreases, contribute to the fluctuations. The curve d is typical of variations where $G(o, \phi, \theta)$ is in a pattern null. Ship motion here causes gain to increase drastically. Curve b demonstrates the opposite effect; the initial smooth-sea observation angle is on the maxima of a lobe and subsequent ship motion causes gain to decrease. The remaining curves, a and c on Figure 4, show cases of the lobes swishing past the observation zenith angle.

III. CONCLUSIONS AND RECOMMENDATIONS

Some tentative conclusions and recommendations may be reached from this study of the mathematical model of shipboard antenna systems in heavy seas:

1. The ionosphere "sees" a time varying gain function at each of the propagation angles. The magnitude and phase of the variations depends upon the particular antenna, ship, sea state, and sea direction. If all variations are additive, the sea state may produce periodic "brightening". If the gain variations are "out of phase", the brightening will occur for different modes of propagation at different times during the period of the wave.

2. The fat lobes of short vertical whips (approximately quarter-wavelength) change the least with ship motion caused by sea state and therefore suggest the use of short vertical whips in heavy weather.

3. High gain antennas, or antennas with multilobed patterns, experience the most radical pattern variations with ship motion. The ionosphere may see drastic changes in gain of all modes and alternate dominance of different modes. These are the most active and most interesting antennas to simulate but will have their usefulness severely limited by heavy seas.

4. Radiation at low angles seems least affected by ship motion. This is the case with both antennas studied

here and also with other types not reported in this document. A trend has definitely been established, but more investigation is warranted. High angle modes, above 35° elevation angle, appear most affected by ship motion. Ionospheric circuits of intermediate or short distances may therefore be most sensitive to sea state.

5. Coding of data for transmission in heavy weather may make high gain antenna systems suitable in an ionospheric circuit. Ship motion is very slow with respect to data rate, suggesting interleaving or some other repetitive encoding scheme with sections arranged to assure transmission during a gain maxima. This would reduce the data rate and would have to be weighed against potential circuit dropouts.

The study of ship motion effects thus far has been speculated on GRAPHANT's model of a flat ocean surface. Some worthwhile experiments could be conducted to verify and quantify these ship motion effects on ionospheric circuits. A short range VHF experiment has been conducted using a vertical quarter-wave monopole aboard the ACANIA, USNPGS Oceanographic Research vessel, to test the usefulness of GRAPHANT at the high end of its intended spectrum. Extension of the math model to include wave profile effects may improve the results but will surely increase the complexity and time of calculation by up to an order of magnitude.

REFERENCES

1. "GRAPHANT - A fortran Program for the Calculation and Graphic Display of Gain and Ratiation Patterns of Wire and Linear Antennas Operating Over Lossy Ground", US Naval Postgraduate School, R. Adler and C. Robbins, June 1972.
2. "The Long-Term Prediction of HF Ionospheric Telecommunications Circuits", Longley, et. al., ESSA-ITS-78, 1969.

T A B L E I

SHIP MOTION FACTORS

For ionospheric communication circuit: 15 Jan 1970
 1298 KM
 MUF = 20.3 MHz₂

Sea state 5

10 M. Vertical Whip

Mode	2E	2E	1F	1F	1F	1F	1F	1F
El. Angle	14.6°	15.9°	17.6°	17.8°	17.9°	18.5°	20.3°	23.3°
Factor	+2db	+2db	+2db	+2db	+2db	+2db	+4db	+10db

7.5 M. Horizontal Dipole, 45 M. high

Mode	2E	2E	1F	1F	1F	1F	1F	1F
El Angle	14.6°	15.9°	17.6°	17.8°	17.9°	18.5°	20.3°	23.3°
Factor	+2.6db	+2.6db	-3.2db	-3.2db	-3.2db	-3.2db	+3db	+10db

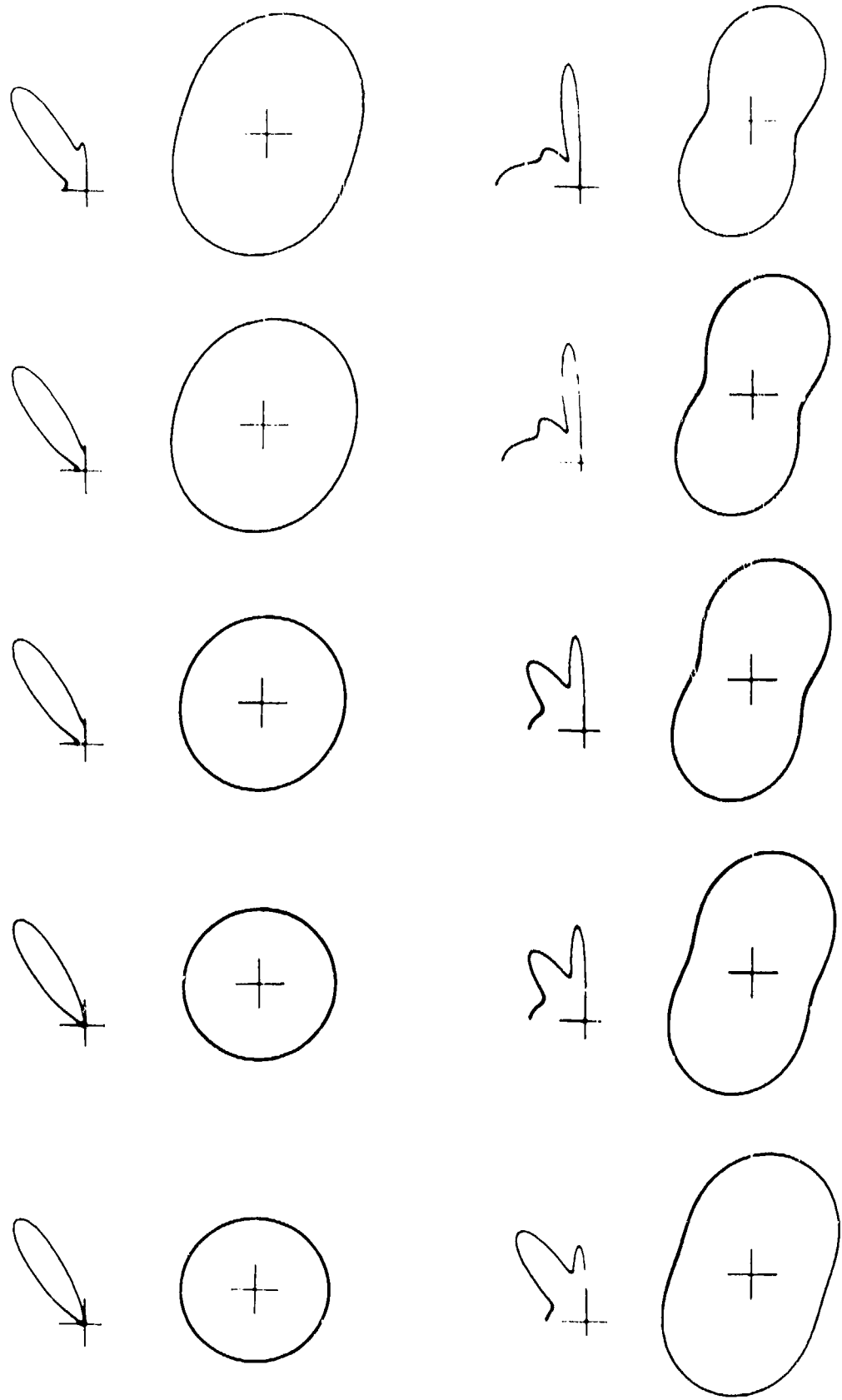


Figure 1. Vertical Thin Radiation Patterns.
 Sea State = 5 from 0450 relative.
 shown every 10° of roll & nitch period.

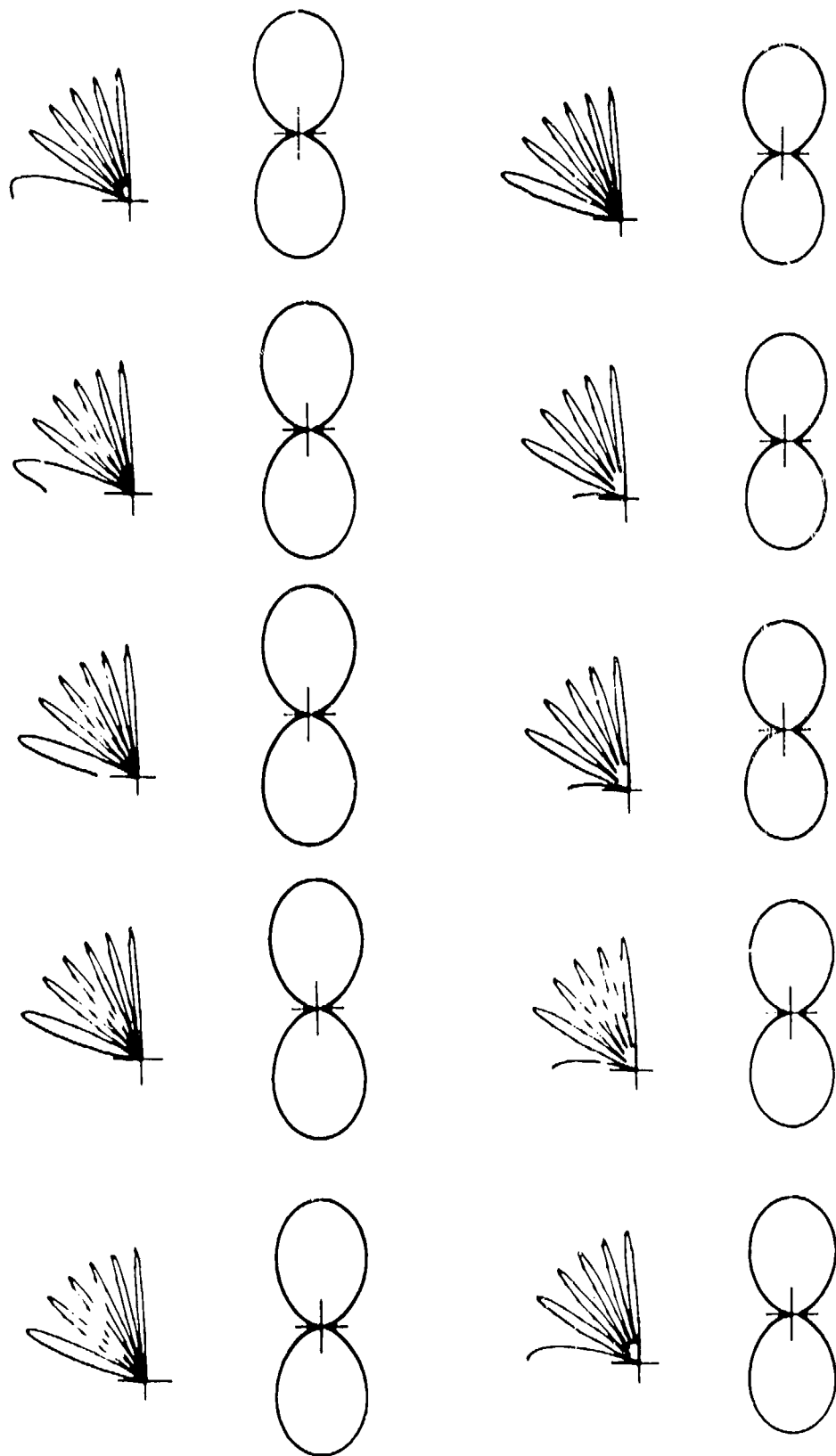
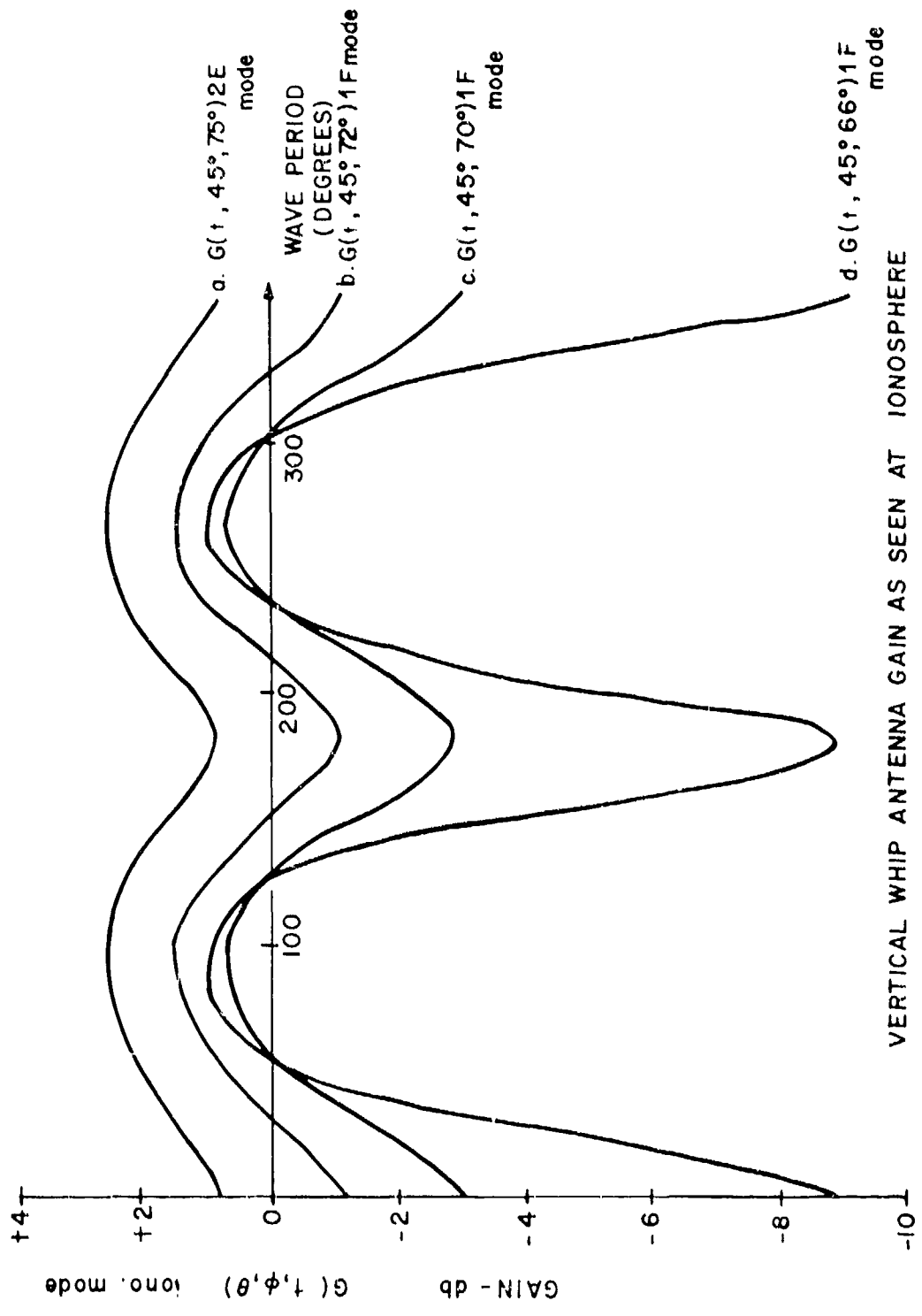
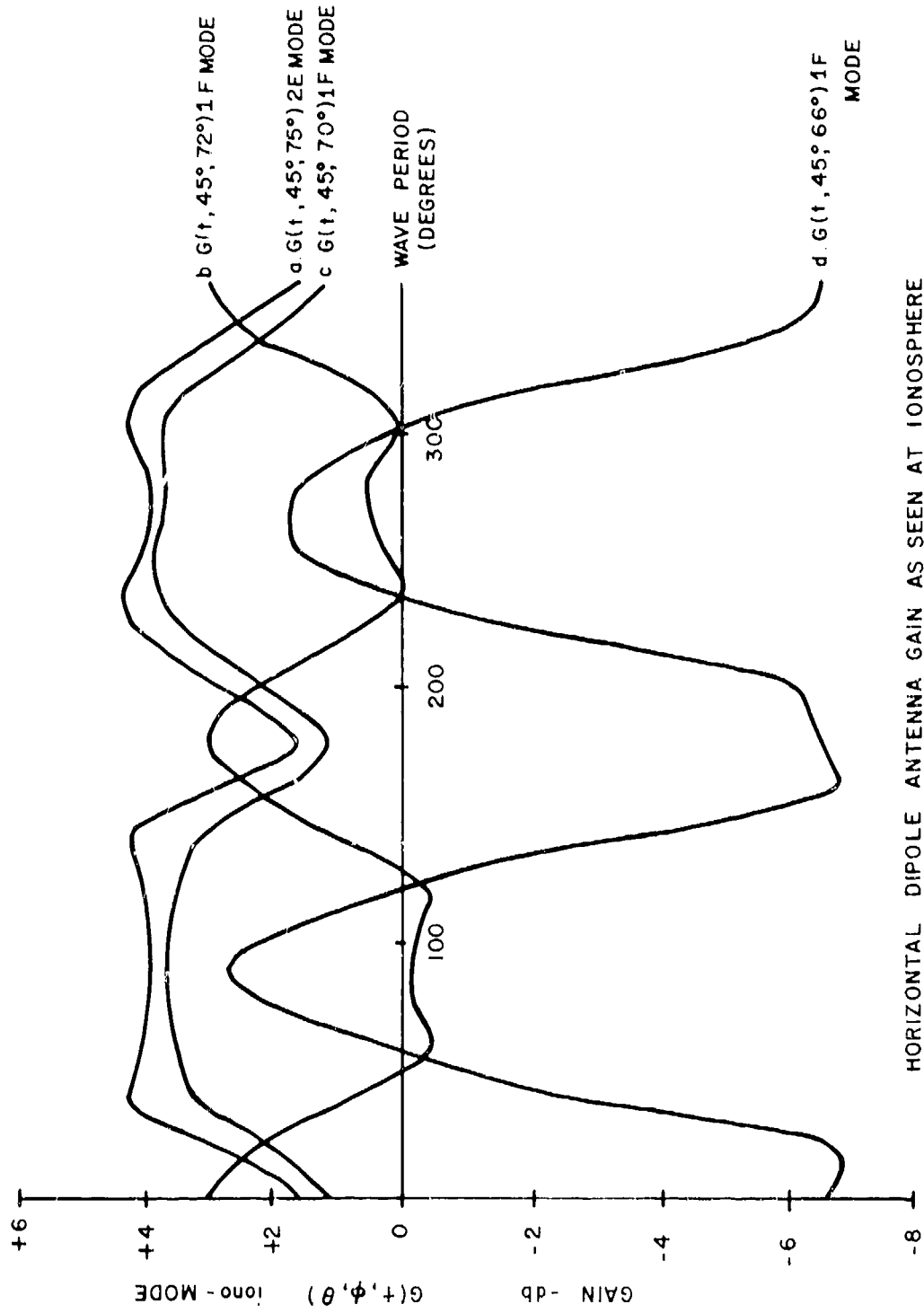


Figure 2. Horizontal Dipole Radiation Patterns.
 See State = 5 from 0.45° relative.
 Shown every 10° of roll & pitch period.

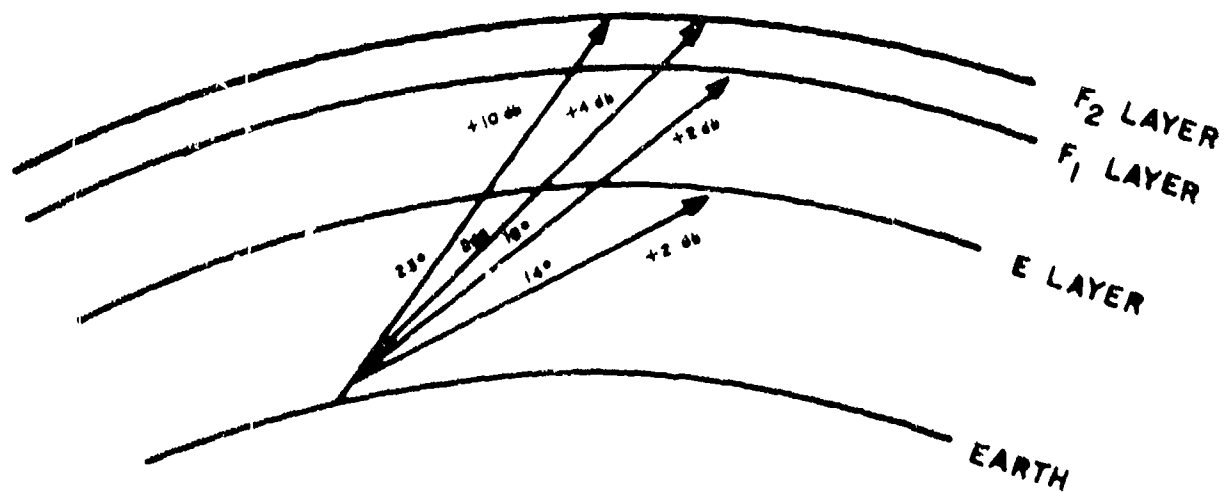


VERTICAL WHIP ANTENNA GAIN AS SEEN AT IONOSPHERE
 FIGURE. 3



HORIZONTAL DIPOLE ANTENNA GAIN AS SEEN AT IONOSPHERE

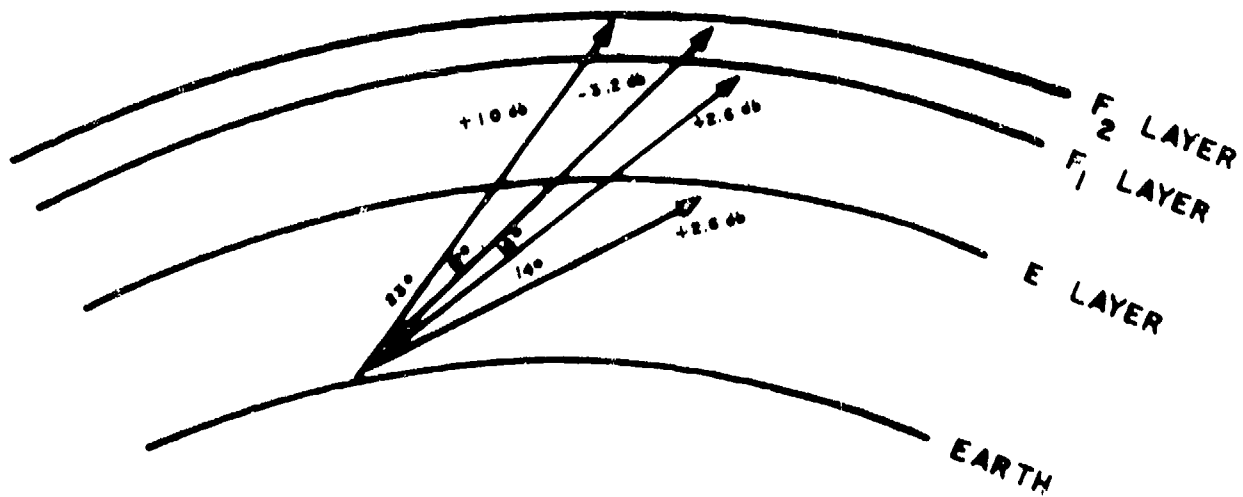
FIGURE 4



SHIP MOTION INDUCED ANTENNA GAIN VARIATIONS FOR
VARIOUS IONOSPHERIC RAYS.

VERTICAL WHIP ANTENNA

Figure 5.



SHIP MOTION INDUCED ANTENNA GAIN VARIATIONS FOR
VARIOUS IONOSPHERIC RAYS.

HORIZONTAL DIPOLE ANTENNA

Figure 6.

S E C T I O N I I I

SEA STATE EFFECTS ON SHIPBOARD VHF ANTENNA PATTERNS

I. INTRODUCTION

The radiation pattern of a shipboard VHF antenna is complicated by the fact that the sea is not a smooth ground plane. In reality the sea is a rough surface which will scatter an incoming wavefront. In addition to this problem, the antenna is not a fixed object in space; it moves in both position and orientation as the ship rolls and pitches. The ship itself is another complicating factor. Even though the ship is electrically insulated from the antenna, interaction occurs, just as there is interaction among reflectors, directors, and the active elements of a yagi antenna. As a result, the shipboard antenna pattern is too complex to be predicted accurately even with the advanced matrix methods of computer solution which have been recently developed.

The number of complicating factors makes approximations necessary. Ultimately then, all attempts to solve the problem of shipboard antenna VHF systems are limited by the approximations made. Even if all approximations are valid, any deterministic solution is doomed to failure due to the randomness of the sea. Some type of probabilistic model is necessary to predict system behavior.

II. THEORY OF THE PROBLEM

A. SIMPLE ANTENNA OVERGROUND

The problem of the vertical stub antenna of length "L" and height "H" above a plane horizontal ground of infinite conductivity can be easily solved by the method of images.¹ The electric field intensity of this system may be defined as a function of elevation angle "α" and distance "r".

$$E(\alpha, r) = \frac{60}{r} \frac{W}{R_{11} + R_{1L}} \frac{\cos(\ell(2\pi/\lambda)\sin\alpha) - \cos(\ell(2\pi/\lambda))}{\cos \alpha}$$

where R_{11} = self-resistance of a vertical stub antenna of length ℓ referred to the point of current maximum

R_{1L} = effective loss resistance of antenna referred to same point

W = power input

In a shipboard VHF communications system the antenna is often located several wavelengths above the sea. When a vertical stub is positioned several wavelengths above the perfect ground plane, the horizontal field pattern remains circular or isotropic, but as the antenna is elevated the vertical pattern will include more and more null and maximum points. That is, as the antenna is elevated the vertical pattern will contain more lobes. This increased number of lobes can

¹Kraus, John D., Antennas, p. 314, McGraw-Hill, 1950.

significantly change received signal strength. A small change in the elevation angle of the incoming signal can cause a large change in received signal strength. This same effect can be expected to occur in shipboard systems.

B. ROTATION OF THE ANTENNA

If the stub antenna over perfect ground is tilted in any direction the field strength pattern will change. This effect can be explained using the pattern multiplication method of analysis. According to this method an antenna array consisting of identical elements is considered to be an arrangement of point sources. The final pattern is the point source pattern multiplied by the element factor. In the case of the tilted stub over ground, the distance between the real and the image point sources will remain the same, but the rotation of the dipole pattern will change the overall field pattern. Thus as a ship rolls and pitches, and therefore the antenna is tilted, two effects take place. One effect is the change in the overall antenna pattern, and the other is the change in the point of entry of the electromagnetic waves on the antenna pattern. These two effects cause large but predictable variations in signal strength. Inherent in this discussion, however, is the smooth surface approximation. The random wave patterns of the sea have not been included.

C. EFFECTS OF A ROUGH GROUND PLANE

Reflection of electromagnetic waves from a smooth surface as used in the previous discussion is a well understood phenomena. In fact, the laws of reflection from a smooth surface are so well known that they are used to determine electrical properties of materials. If the surface is rough, however, the electromagnetic energy will be scattered in various directions. To predict the form of the scattered field is a very difficult problem. This phenomenon has received particular attention in connection with radio propagation in the VHF range. In line-of-sight communication systems the field at the receiving point may be broken up into a direct and a reflected ray. In the case of a smooth earth the field pattern may be easily predicted as in the previous discussion of the tilted stub. When the surface is rough the problem rapidly expands. Since the surface of the sea is time varying, an exact solution is not possible. The received signal will be subject to fades which are determined by the form and movement of the sea. In analyzing random rough surfaces the surface is normally assumed to isotropically rough. That is, the surface is assumed to have the same statistical distribution in all directions over the surface. When the surface distribution is different in the X and Y directions, the calculation becomes very involved. This case of an isotropic roughness occurs for the

surface of the sea which may have a different distribution on and across the direction of the wind.²

D. THE SEA AS A GROUND PLANE

The surface of the sea has been subject of many theoretical and experimental investigations. Schooley [1954] and Cox and Munk [1954] have measured the distribution of the slopes of the surface of the sea by optical methods. According to Cox and Munk this distribution is to a first approximation a normal type distribution. The standard deviation of this distribution is a function of the wind-speed. Their investigation also indicates that the slopes of the waves were higher in the upwind direction. This means that the sea is not isotropic. The distribution of wave slopes derived from measurement of back-scatter of radar pulses and by optical methods are in agreement. In both cases the distribution is normal.³ Information obtained to date indicates that to a second approximation the wave slopes are slightly asymmetrical and they depend upon the direction of the wind. Thus although the mechanism by which the sea scatters an electromagnetic wave is known, the sea surface is not known well enough to predict at any instant what the signal strength will be.

²Beckman, P., and Spizzichino, A., The Scattering of Electromagnetic Waves from Rough Surfaces, p. 405, MacMillan, 1963.

³Ibid., p. 409.

E. THE COMPOSITE PICTURE

Major signal strength variations will occur as indicated previously due to the roll and pitch of the antenna. In addition to these variations there is a randomness in the variations due to scatter from the sea. As the ship rolls to one side, the signal strength will not always move to the value predicted by the smooth surface approximation, it will be offset by some value determined by the sea reflections at that instant. Thus, signal strength will vary to a band of values. The means of this band should be determined by the degree of roll and pitch, and the variance of the band should depend upon wind conditions.

III. EXPERIMENTAL PROCEDURE

A. EQUIPMENT SET UP

1. Antenna properties

In order to reduce the number of variable factors included in the collection of data the antenna used was nearly isotropic in the horizontal plane. If a non-isotropic antenna had been used all data would also have been dependent upon the antenna pattern in the direction of the source. In the vertical plane the antenna pattern had many lobes since the problem required that it be many wavelengths above ground. A quarter wavelength vertical element over a ground plane was chosen for its simplicity and its ability to meet problem requirements. The ground plane consisted of four aluminum radial elements. The antenna was designed using published curves.⁴ The elements were trimmed and the radials bent to tune the antenna to match a 50 ohm transmission line at 149.13 MHz. The final design consisted of an active vertical element 47.65 cm long. The ground plane consisted of four radial elements 47.7 cm long. The radials were bent down 45° from the horizontal.

2. Research Vessel Acania

The antenna was mounted aboard the research vessel Acania. The mounting point was the highest point of the ship, 60 feet above the waterline. The Acania is operated

⁴Jasik, H., Antenna Engineering Handbook, p. 14, McGraw Hill, 1961.

under the sponsorship of the Oceanographer of the Navy by a five man civilian crew employed by the Naval Postgraduate School. The vessel is 126 feet overall with a beam of 21 feet 4 inches. Under normal operating conditions it displaces 246.8 gross tons. The Acania's small size made it an excellent platform for this experiment.

3. Recorder and Receiver

The receiving equipment consisted of an AN/URR-27 radio receiver connected to a Hewlett Packard #680 strip recorder. The URR-27 is designed to receive an amplitude modulated voice transmission in the 105-190 MHz frequency range. The receiver was crystal tuned to 149.13 MHz to avoid the drift problems encountered in the manual tuning mode. The transmitted signal was CW only. The basic receiver was modified for this experiment by disconnecting the AVC bus from the "IF" amplifiers. The strip recorder was connected from the AVC bus to an external power supply which was grounded to the receiver. This resulted in an output on the strip recorder that was approximately linearly related to the input CW signal.

IV. EXPERIMENTAL RESULTS

A. RECORDED DATA

Received signal strength was continuously plotted on the strip recorder as the ship steamed from point to point. Along with the continuous signal strength plot, the ships course and speed, and the direction and distance of the radiating source were periodically recorded. Only a rough estimate of roll and pitch using the ship's inclinometer could be obtained.

Typical recorded signal strengths are shown in Figures 1 through 3. The sea conditions were combinations of two situations: choppy surface and large swells. Figure 1 is for chop without swells and shows a rapid 1db fluctuation. For the case of no chop but large swells in Figure 2, the variation is about 5db. Figure 3 shows the combination case of approximately 6db variation.

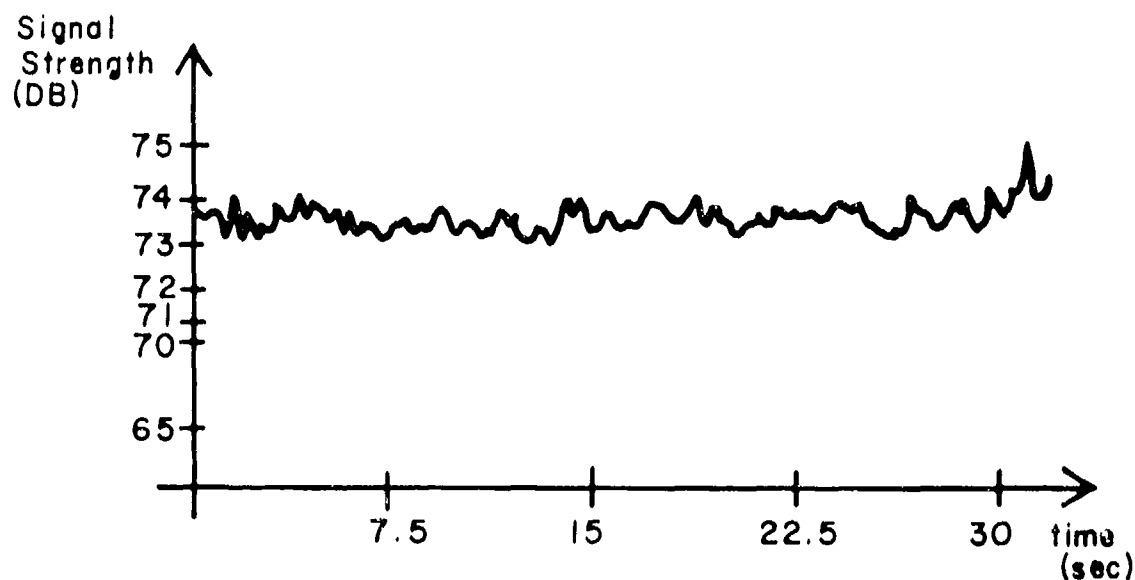


Figure 1. Signal Variations Over a Choppy Sea With No Large Swells.

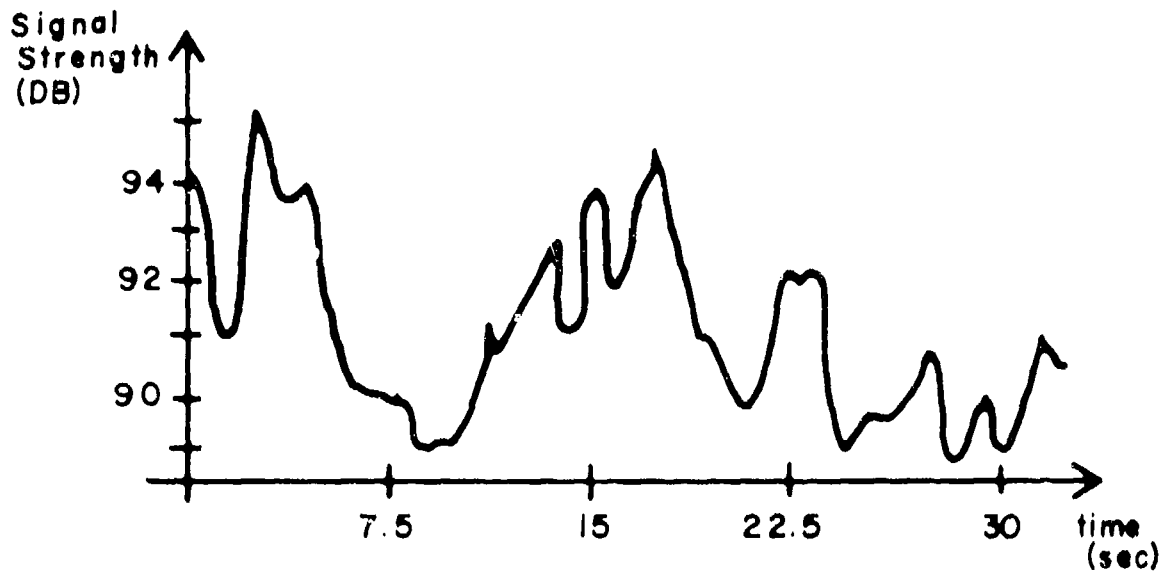


Figure 2. Signal Variations Over a Sea with Large Swells but No Choppiness.

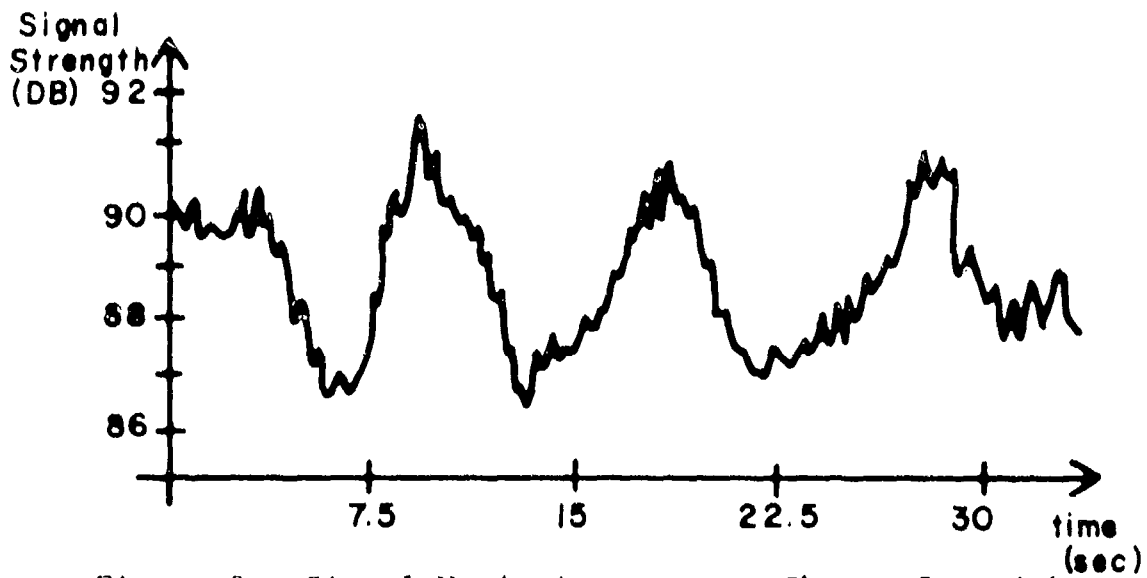


Figure 3. Signal Variations over a Choppy Sea with Large Swells.

B. COMPUTER SIMULATION

1. Program Set Up

The computer simulation of the problem was programmed for use on the AGT-10 graphics terminals. The basic equations used were taken from two technical reports, "Predicting Long-Term Operational Parameters of High-Frequency Sky Wave Telecommunication Systems" (ESSA-ERL-110-ITS78) and "Power Gains for Antennas Over Lossy Plane Ground" (ESSA-ERL-104-ITS74). The programs predict how antenna patterns will vary as a ship rolls and pitches over a smooth sea surface. The first parameter that must be input on the graphics terminal is the antenna type. A vertical monopole, inverted L, sloping long wire, vertical monopole with ground screen, vertical half rhombic or a dipole may be chosen. Next antenna length, height above the sea, and orientation on the ship are input. Other inputs establish frequency, direction of the incoming signal, and environmental constants. The program outputs a plot of the vertical and horizontal antenna patterns at the point designated, incoming signal strength, and maximum roll and pitch angles. The ship rolls from an upright position, to a maximum roll and pitch, through upright to the other maximum, and back to upright in thirty six equal intervals. Data is output for the antenna orientation on each interval.

V. COMPARISON OF RESULTS

A. DISTRIBUTIONAL ANALYSIS

A distributional analysis of the recorded data showed, as expected, two peaks of signal strength with a decrease to the mean value of the incoming signal in between the peaks. No relationship between the pitch & roll conditions and the peaks of the analysis was obvious.

B. VARIATIONAL ANALYSIS

A variational analysis followed closely the results of the distributional analysis. The average value was zero, showing that the data runs were short enough so that the average signal strength was constant. The peaks here also did not correlate with pitch and roll.

C. SIMULATION ANALYSIS

The computer simulation did not include all of the randomness of the sea & thus did not predict where peaks in the distributional & variational analyses occurred. The calculated data contained more peaks than did the measured data. The rough surface seemed to smooth out the antenna pattern at this VHF frequency and make it more predictable in that only one average value of signal occurred.

2. Computer Results

Typical of the many calculated cases is the data shown in Tables 1 & 2. The signal variations predicted by the idealized plane-surfaced ocean were 3.5 to 4 db, based on the same roll & pitch as estimated by the experimental runs.

ANTENNA SIMULATION

LENGTH OF ANTENNA = .95 METERS
 HEIGHT OF ANTENNA = 18.2 METERS
 PHI OF ANTENNA = 000 DEGREES RELATIVE
 THETA OF ANTENNA = 000 DEGREES RELATIVE
 FREQUENCY = 149.0 MHZ
 EPSILON = 80.0
 SIGMA = 5.0
 PHI OF PLOT = 306 DEGREES RELATIVE
 THETA OF PLOT = 089 DEGREES RELATIVE
 SEA STATE = 2
 DIRECTION OF SEA = 018 DEGREES RELATIVE

ROLL (DEGREES)	PITCH (DEGREES)	SIGNAL STRENGTH (DB)
.9	.0	4.875
1.7	.0	1.452
2.5	.0	1.490
3.2	.0	2.809
3.8	.0	3.353
4.3	.0	2.852
4.6	.0	2.319
4.9	.0	2.058
4.9	.0	1.989
4.9	.0	2.058
4.6	.0	2.319
4.3	.0	2.852
3.8	.0	3.353
3.2	.0	2.809
2.5	.0	1.490
1.7	.0	1.452
.9	.0	4.875
-.9	.0	5.080
-1.7	.0	1.592
-2.5	.0	1.416
-3.2	.0	2.594
-3.8	.0	3.332
-4.3	.0	3.054
-4.6	.0	2.564
-4.9	.0	2.275
-4.9	.0	2.190
-4.9	.0	2.275
-4.6	.0	2.564
-4.3	.0	3.054
-3.8	.0	3.332
-3.2	.0	2.594
-2.5	.0	1.416
-1.7	.0	1.592
-.9	.0	5.080

AVERAGE VALUE = 2.66 DB

Table 1 - Computer-simulated Run (Roll only)

ANTENNA SIMULATION

LENGTH OF ANTENNA ▪ .95 METERS
 HEIGHT OF ANTENNA ▪ 18.2 METERS
 PHI OF ANTENNA ▪ 000 DEGREES RELATIVE
 THETA OF ANTENNA ▪ 000 DEGREES RELATIVE
 FREQUENCY ▪ 149.0 MHZ
 EPSILON ▪ 80.0
 SIGMA ▪ 5.0
 PHI OF PLOT ▪ 184 DEGREES RELATIVE
 THETA OF PLOT ▪ 089 DEGREES RELATIVE
 SEA STATE ▪ 5
 DIRECTION OF SEA ▪ 007 DEGREES RELATIVE

ROLL (DEGREES)	PITCH (DEGREES)	SIGNAL STRENGTH (DB)
.8	2.6	4.967
1.7	5.2	1.477
2.4	7.5	1.364
3.1	9.7	2.547
3.7	11.6	3.224
4.2	13.1	2.913
4.6	14.2	2.408
4.8	14.9	2.101
4.9	15.1	2.008
4.8	14.9	2.101
4.6	14.2	2.408
4.2	13.1	2.913
3.7	11.6	3.224
3.1	9.7	2.547
2.4	7.5	1.364
1.7	5.2	1.477
.8	2.6	4.967
-.8	-2.6	5.168
-1.7	-5.2	1.618
-2.4	-7.5	1.298
-3.1	-9.7	2.320
-3.7	-11.6	3.122
-4.2	-13.1	3.043
-4.6	-14.2	2.634
-4.8	-14.9	2.337
-4.9	-15.1	2.239
-4.8	-14.9	2.337
-4.6	-14.2	2.634
-4.2	-13.1	3.043
-3.7	-11.6	3.122
-3.1	-9.7	2.320
-2.4	-7.5	1.298
-1.7	-5.2	1.618
-.8	-2.6	5.168

AVERAGE VALUE = 2.63 DB

Table 2 - Computer-simulated Run (Roll & Pitch)

VI. CONCLUSIONS

As a ship rolls and pitches, signal strength will, on the average, vary between two values. The magnitude of these variations is dependent first of all upon sea state, since this determines the height of the large ocean swells. The variations also depend upon wind speed since this determines choppiness. A third dominant factor is the relative direction from which the signal is being received. A smooth surface approximation is not justified since the rough surface reflections have a smoothing effect on the antenna pattern which modifies the magnitude and the frequency of the variations.